Available online at www.sciencedirect.com
SCIENCE DIRECT
ELSEVIER
Journal of Membrane Science xxx (2006) xxx–xxx
journal of MEMBRANE SCIENCE
www.elsevier.com/locate/memsci

Influence of porous substrate on mesopore structure and water permeability of surfactant templated mesoporous silica membranes

Sankhanilay Roy Chowdhury [1], Alisia M. Peters, Dave H.A. Blank, Johan E. ten Elshof *

Inorganic Materials Science, MESA+ Institute for Nanotechnology and Faculty of Science and Technology, University of Twente, P.O. Box 217, 7500 AE Enschede, The Netherlands

Received 5 September 2005; received in revised form 4 December 2005; accepted 7 December 2005

Abstract

The formation of silica films via sol–gel route on disordered mesoporous and macroporous supports is reported. These films are structurally characterised by TEM, XRD, XPS and permporometry. It has been found that the ordered mesoporous silica layer does not grow directly on a mesoporous support. Instead it grows on a structurally disordered interface of 10–20 nm thickness. This observation differs considerably from studies on film formation on dense supports as reported in the literature. Water transport experiments were carried out on the silica films deposited on porous supports. The results suggest that the disordered interface layer of the film deposited on the mesoporous support does not contribute significantly to the total resistance for water transport.

Keywords: Membrane; Mesoporous; Silica; Mesostructured material; Permeability

1. Introduction

Since the first development of surfactant templated MCM-type silica materials [1], ordered mesoporous silica systems achieved a lot of attention of scientists from different fields [2–4]. In the 1990s the effort was mostly given to the preparation and characterization of surfactant templated silica powders and thin films [5,6]. Powders were prepared from different silica sources, using different types of surfactants to achieve regular pore geometries [7,8]. Thin films were made either in self-supported form or were supported by different dense substrates [6–13]. Edler and Roser has published a comprehensive review on surfactant templated silica films [14]. In the last few years a considerable amount of work on the application of ordered mesoporous silica layers as membranes was reported [15–24]. This dealt with the formation of mesoporous silica films on macroporous supports [15,16] and preparation of defect-free mesoporous silica layers on macroporous supports through temporary modification of the support [17]. Zirconia-doped silica membranes to get an alkali resistance membrane has also been reported [18]. These mesoporous silica membranes have been used for gas permeation and separation [19,20], pervaporation [21], ultrafiltration and nanofiltration [19–24].

In this article we describe the preparation of surfactant templated silica layers on disordered mesoporous and macroporous supports. A detailed structural characterization of these layers has been carried out. We are able to show that both X-ray diffraction (XRD) and transmission electron microscopy (TEM) measurements can be carried out directly on the membrane surface. The water permeability through the layers was measured and this allowed us to establish a correlation between the layer structure and the water transport properties.

2. Experimental

2.1. Membrane preparation

The silica sol synthesis was carried out as described by Honma et al. [25]. In this method, 8.0 ml of silica source

* Corresponding author. Tel.: +31 53 489 2695; fax: +31 53 489 4683.
E-mail address: j.e.tenelshof@utwente.nl (J.E.t. Elshof).
[1] Present address: Ecole Nationale Supérieure de Chimie Mulhouse, 3, Rue Alfred Werner, 68093 Mulhouse Cedex, France.

0376-7388/$ – see front matter © 2005 Elsevier B.V. All rights reserved.
doi:10.1016/j.memsci.2005.12.015

tetraethoxyorthosilicate (TEOS) (Aldrich, purity 99%) was mixed with 17.5 ml 1-propanol, and this mixture was stirred in a 100 ml flask at 600 rpm for 5 min. The TEOS was then hydrolysed by an HCl solution in deionised water (0.33 ml 36 (N) HCl solution in 2 ml water) and stirred for 60 min. Co-solvent 2-butanol (8.8 ml) was added and stirring was continued for another 30 min. In the last step, 1.75 g of CTAB was dissolved in 4.5 ml of de-ionized water. This surfactant solution was prepared separately and then poured into the silica solution. The final solution was stirred again for 60 min. The sol was deposited on two different types of substrates with varying degree of porosity. α-Alumina and α-alumina supported γ-alumina disks were used as macroporous and mesoporous supports, respectively. The preparation of these supports has been described elsewhere [26]; the γ-alumina layer was calcined at 900 °C. The porosity of macroporous α-alumina supports is ∼30% and the average pore size is in the range of 80–120 nm. The porosity of the γ-alumina layer is ∼55% with an average pore radius of ∼4.3 nm, and its layer thickness on the α-alumina support is 3 μm.

The silica sols were coated twice on both the α-alumina disks and the α-alumina supported γ-alumina layers using the dip coating technique, with a coating speed of approximately 1 cm s^{-1}. The silica coated supports were calcined at 450 °C for 90 min in air with heating and cooling rates of 0.2 °C min^{-1}.

2.2. Structural characterization of supported silica layers

The supported silica films were characterized by X-ray diffraction (XRD), transmission electron microscopy (TEM), electron diffraction (ED), and permporometry. XRD was carried out directly on supported membranes using a Philips SR5056 with Cu Kα radiation. Transmission electron microscopy (TEM) and electron diffraction (ED) were carried out with a Philips CM30 Twin (S)TEM with a LaB_6 filament. A 120–200 kV electron beam was used for TEM. The samples for TEM were prepared by sandwiching and glueing the membrane, followed by cutting them vertically into slices of 1 mm thickness. These were mechanically polished in several steps to 90 μm thickness, followed by grinding with a dimpling wheel down to a thickness of ∼15 μm. Finally, the samples were thinned by Ar^+ ion milling (Gatan model 691 Precision Ion Polisher, 5.0 keV) under an angle of 4.5° to minimize damage.

The pore size distribution of the supported silica layers was determined by permporometry measurements using cyclohexane as condensable vapor [27]. The method was also used to check for the absence of large pores and/or other defects in the film. X-ray photoelectron spectroscopy (XPS) was carried out with a PHI Quantum 2000 Scanning ESCA Microprobe. XPS depth profiling of the α-alumina supported silica layer was carried out with a 3 keV argon ion beam with an etching rate of 7 nm min^{-1}.

2.3. Water permeation experiments

Steady state water permeability measurements were carried out in a dead end filtration cell with different membranes. The membranes used for this experiments were an α-alumina support, an α-alumina supported γ-alumina membrane, an α-alumina supported double coated silica membrane, and α-alumina/γ-alumina supported double coated silica membranes. The volume of the filtration cell was 1 dm^3 and the operating pressure range was kept in the range of 2–14 bar. Liquid stirring was done with a mechanical stirrer at a constant stirring speed of 200 rpm throughout the permeation experiments.

3. Results and discussion

3.1. Structural characterization

Permporometry experiments were carried out on silica layers supported on α-alumina and on α-alumina supported γ-alumina membrane discs. Fig. 1 shows the oxygen flux through open pores versus the relative vapor pressure of cyclohexane. In the absence of cracks or large defects in the layer, the oxygen flux is zero at relative cyclohexane pressures above 0.5. This indicates that no pores with Kelvin radii larger than approximately 1.5 nm are present in the membranes. Hence, the layers derived from the silica sol on both macroporous and mesoporous supports were defect-free. The figure also illustrates the microporous nature of the silica layer on macroporous supports. As the Kelvin equation is not valid for microporous systems, no reliable pore size distribution can be calculated from the permporometry measurements on this system. The cyclohexane saturation point at a relative pressure of ∼0.3 corresponds with an average pore radius of approximately 0.9 nm. The oxygen flux through the silica membrane supported on an α-alumina supported γ-alumina layer shows three different regions with varying cyclohexane pressure. When the relative pressure was higher than ∼0.4, all pores were blocked by condensed cyclohexane and no oxygen flux was observed. Reduction of the relative pressure from 0.4 to 0.3 led to a strong increase of the oxygen flux, due to desorption of cyclohexane from the pores in the capillary condensation regime. A further decrease in relative pressure resulted in a slight increase of the oxygen flux. This is thought to be mainly due to the (partial) desorption of the *t*-layer inside the pores. The

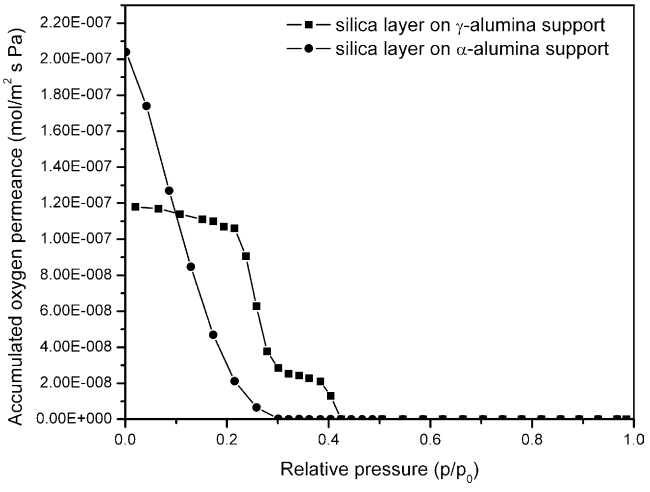

Fig. 1. Oxygen flux vs. relative vapor pressure of cyclohexane through silica layers deposited on α-alumina and on γ-alumina.

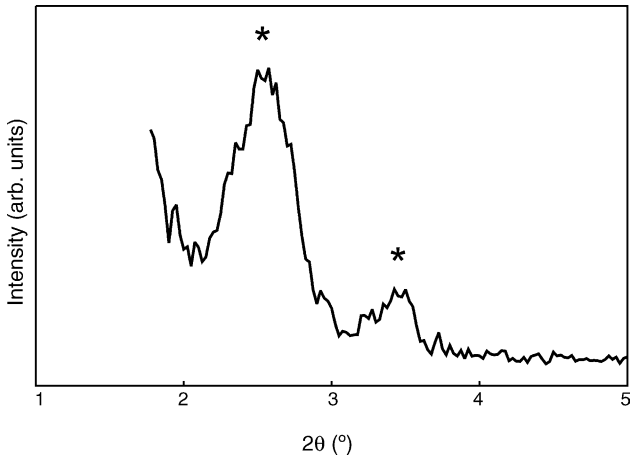

Fig. 2. XRD diagram of a double silica layer deposited on a γ-alumina substrate layer after calcination.

cyclohexane saturation point at a relative pressure of ∼0.4 corresponds to an average pore radius of ∼1.2 nm.

The silica membranes supported by α-alumina and γ-alumina were subjected to XRD analysis. The layer deposited on α-alumina did not reveal any diffraction peaks in the 2θ range of 0–10°, which may be caused by the small thickness (∼250 nm) of this layer [15,23]. However, the layer deposited on γ-alumina supports showed clear peaks around 2.5° and 3.4°, as shown in Fig. 2. These are characteristic of an ordered mesoporous structure [18].

A TEM micrograph of the γ-alumina supported silica layer is shown in Fig. 3A. A superstructure is clearly visible in the silica layer. It has a periodicity of about 4 nm, and was found to be oriented in different directions in different mesoscopic domains along the γ-alumina interface. An interfacial layer of 10–20 nm thickness can be observed in between the ordered silica layer and the γ-alumina substrate layer. Dark field imaging (not shown) indicated that this interface layer has an amorphous structure. EDX point analyses in the centre of the silica film, the γ-alumina film, and the α-alumina substrate yielded atomic concentrations as listed in Table 1. The electron beam diameter in this experiment was approximately 6 nm. From the EDX line scans it could be concluded that the interfacial layer consists mainly of silica. Together with the results from TEM contrast imaging and morphology, it is reasonable to assume that the amorphous interfacial region has a similar chemical composition as the ordered mesoporous SiO_2 film. As can be seen from the enlarged TEM picture in Fig. 3B, in the first few nanometers of the ordered silica phase, there appears to be an alignment parallel to the amorphous interfacial layer. Apparently, the ordered silica layer does not grow directly on top of the γ-alumina layer outwards starting from the γ-alumina/silica interface. In that case the highest degree of ordering is expected to occur near the interface at which growth starts [28]. Instead, there is a structurally disordered interfacial region of about 15 nm thickness located between the silica and γ-alumina layers. Growth of the ordered phase appears to occur outwards from the disorded–ordered silica interface. A possible explanation for this phenomenon may be as follows. At the time of dip coating the silica sol comes into contact with the mesoporous γ-alumina substrate. The γ-alumina pores of ∼4.3 nm radius may exert a very large capillary suction pressure on the sol liquid. The pressure $\Delta P_{\text{suction}}$ is of the order

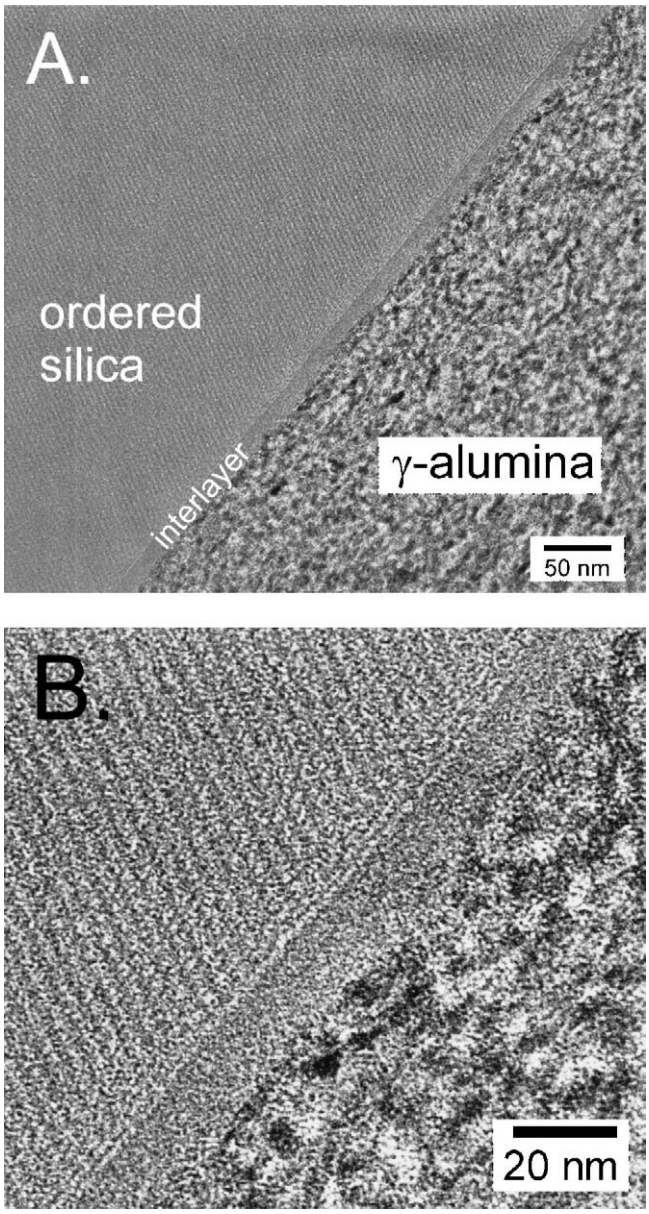

Fig. 3. (A) TEM image showing an ordered silica layer on a mesoporous γ-alumina layer with a structurally disordered silica-rich interface of 10–20 nm thickness; (B) enlarged TEM image showing ordering of silica layer parallel to the interlayer.

Table 1
Atomic compositions of different layers of a supported silica membrane deposited on a γ-alumina layer

Layer	O (at.%)	Al (at.%)	Si (at.%)
Mesostructured silica	66.4	1.7	31.9
Interfacial layer	66.1	1.4	32.5
γ-Alumina	61.1	33.2	5.7
α-Alumina	60.0	39.8	0.2

Data determined from EDX point analyses.

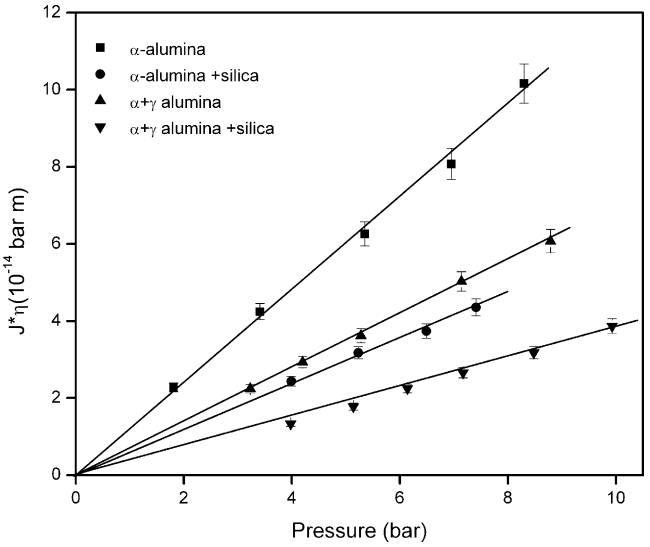

Fig. 4. Product of water flux and viscosity vs. applied pressure of different membranes.

$2\gamma_l/r$, with γ_l and r the surface tension of the sol and pore size of the γ-alumina phase, respectively. Hence $\Delta P_{suction}$ is about 10–25 MPa. The suction by the support may enhance the drying rate of the silica film near the interface so drastically that the silica framework freezes before any self-organization has occurred. The suction force is also sufficiently large to cause turbulence locally, disrupting any ordered micellar domains, resulting in no ordered mesostructure near the interface. As soon as the γ-alumina capillaries near the surface are saturated by the sol liquid, the suction force vanishes and further growth of the silica structure can take place in the form of an ordered structure on top of the interface. This mode of growth differs from what is commonly reported in literature, namely that ordered silica layers grow directly on the dense substrate, with growth starting at the interface [29]. The experiment that we present here suggests that film formation may be quite different on porous substrates.

3.2. Water transport through the silica layers

The steady state water fluxes through an α-alumina support, an α-alumina supported γ-alumina membrane, γ-alumina supported silica membranes, and an α-alumina supported silica layer are shown in Fig. 4. According to Darcy's law, when the transport mechanism obeys the viscous flow model, the liquid flux is proportional to the applied pressure, irrespective of the type of liquid. The mathematical formulation of Darcy's law is:

$$J = -\frac{1}{\eta} k_m \Delta P \quad (1)$$

where J is the volumetric flux, η the liquid viscosity, ΔP the applied pressure difference across the membrane and k_m is the overall liquid permeability of the membrane. The ratio $J/\Delta P$ is commonly referred to as the permeability of a membrane. For the two membranes with a silica top layer the permeability varied between ∼1.5 and ∼2.4 L m^{-2} h^{-1} bar^{-1}. This is in good agreement with the permeability of a supported MSU-type silica membrane with similar pore size and layer thickness, where a permeability of 2.5 L m^{-2} h^{-1} bar^{-1} (at 10 bar) was reported [15].

The overall transport resistance of liquids through a stacked α-alumina/γ-alumina or α-alumina/γ-alumina/silica membrane can be regarded as two (or three, depending upon the number of layers) resistances in series. The overall membrane permeability coefficient k_m can therefore be deconvoluted into the permeabilities of the individual layers according to:

$$k_m^{-1} = k_\alpha^{-1} + k_\gamma^{-1} + k_{Si}^{-1}, \quad (2)$$

where k_α, k_γ and k_{Si} are the permeability coefficients of the α-alumina support, the mesoporous γ-alumina layer, and if present, the silica top layer, respectively. Table 2 summarizes the permeability coefficients (k_p) for water of the individual layers after deconvolution.

To compare the intrinsic permeabilities of the different porous structures (i.e. independent of the actual layer thickness), the product k_pL was calculated. From TEM analysis and XPS depth profiles of silica layers deposited on γ-alumina and α-alumina we know that the silica layers have thicknesses L of ∼600 and ∼250 nm, respectively. Comparison of the k_pL values in Table 2 indicates that the γ-alumina pore structure is more permeable than the silica films. However, the γ-alumina layer has an average pore radius of ∼4.3 nm, while we can estimate the pore radii of the γ-alumina and α-alumina supported silica layers from permporometry experiments to be ∼1.2 and ∼0.9 nm, respectively. Under conditions where Darcy's law is valid, the permeability coefficient of a single layer k_p with pore radius r is given by:

$$k_p = \frac{\varepsilon r^2}{8\tau L} \quad (3)$$

Table 2
Calculated permeability coefficients k_p of different individual layers from stacked membranes

Layer	Support	L (μm)	k_p ($\times 10^{-14}$ m)	k_pL ($\times 10^{-20}$ m^2)	ε (%)	r_p (nm)	τ
γ-Alumina	α-Alumina	3.0	1.68 ± 0.01	5.0	55	4.3	∼25
Silica	γ-Alumina	0.60	0.79 ± 0.05	0.47	58	1.2	∼22
Silica	α-Alumina	0.25	1.19 ± 0.07	0.29	58	0.9	∼21

Corresponding layer thicknesses L as determined from SEM and XPS depth profiling experiments; porosity ε estimated from nitrogen sorption data [13,26]; pore radii determined from permporometry experiments and tortuosity τ calculated using Eq. (3).

where ε is the porosity of the membrane material and τ is the tortuosity of the pore structure [30]. We showed recently that Darcy's law is valid down to pore radii of 1.6 nm or smaller when water is used as the permeating medium [31], and we assume here that it is still valid down to pore radii of ~1 nm. Taking the porosities of γ-alumina and the silica layers as 55% [26] and 58% [13], respectively, the tortuosities τ of the individual layers can be estimated from Eq. (3). The results are shown in Table 2. Irrespective of the actual physical significance of the tortuosity, it expresses an effective coefficient of resistance against diffusion. The tortuosities of the γ-alumina and silica layers are similar within experimental error. The tortuosity of the γ-alumina layer agrees reasonably well with earlier findings [32]. The high tortuosities of the two silica layers indicate that no highly permeable pore structures were formed in either case. This can possibly result from a lack of connected mesoporosity, and/or an unsuitable orientation of the mesopores (alignment parallel to the surface instead of through-surface). In any case, the permeability differences between the layers can be fully explained by differences in layer thickness, pore size and porosity. Since the two silica layers have similar permeabilities, this result also suggests that the structurally disordered interface layer does not have a significant resistance for water permeation through γ-alumina supported silica membranes.

4. Conclusions

Silica films deposited on a mesoporous support showed ordered mesoporous domains, but the films deposited on a macroporous support did not. Defect-free layers could be formed both on macroporous and mesoporous supports. The ordered silica layer was shown not to grow directly on a mesoporous substrate. Instead a structurally disordered thin silica interface of 10–20 nm thickness was formed on the substrate, on top of which a mesostructured mesoporous silica layer of 600 nm thickness formed. Water transport experiments suggest that the permeability of the disordered interface layer does not contribute significantly to the total resistance of the membrane to transport of water.

The formation of a disordered interface can be explained by the effect of capillary suction by the support, which is probably so large that it could enhance the drying rate of the silica phase near the interface to such an extent that the silica framework forms before self-organization of CTAB can actually occur. If this hypothesis is correct, one could minimize or avoid the formation of a disordered interface by maintaining a certain level of moisture in the substrate while coating the templated silica layer, so that the pores of the substrate are filled and no capillary suction can occur.

Acknowledgment

Financial support of the Commission of the EC in the framework of the Growth Program, contract no. G1RD-2000-00347 (SUSTOX) is gratefully acknowledged.

References

[1] J.S. Beck, J.C. Vartuli, W.J. Roth, M.E. Leonowicz, C.T. Kresge, K.D. Schmitt, C.T.-W. Chu, D.H. Olson, E.W. Sheppard, S.B. McCullen, J.B. Higgins, J.L. Schlenkert, A new family of mesoporous molecular sieves prepared with liquid crystal templates, J. Am. Chem. Soc. 114 (1992) 10834.
[2] M. Grun, A.A. Kurganov, S. Schacht, F. Schuth, K.K. Unger, Comparison of an ordered mesoporous aluminosilicate, silica, alumina, titania and zirconia in normal-phase high-performance liquid chromatography, J. Chromatogr. A 740 (1996) 1.
[3] P.D. Yang, G. Wirnsberger, H.C. Huang, S.R. Cordero, M.D. McGehee, B. Scott, T. Deng, G.M. Whitesides, B.F. Chmelka, S.K. Buratto, G.D. Stucky, Mirrorless lasing from mesostructured waveguides patterned by soft lithography, Science 287 (2000) 465.
[4] K. Kageyama, J. Tamazawa, T. Aida, Extrusion polymerization: catalyzed synthesis of crystalline linear polyethylene nanofibers within a mesoporous silica, Science 285 (1999) 2113.
[5] K. Schumacher, P.I. Ravikovitch, A. Du Chesne, A.V. Neimark, K.K. Unger, Characterization of MCM-48 materials, Langmuir 16 (2000) 4648.
[6] V. Alfredsson, M.W. Anderson, Structure of MCM-48 revealed by transmission electron microscopy, Chem. Mater. 8 (1996) 1141.
[7] Q.S. Huo, R. Leon, P.M. Petroff, G.D. Stucky, Mesostructure design with gemini surfactants—supercage formation in a three-dimensional hexagonal array, Science 268 (1995) 1324.
[8] F.X. Chen, L.M. Huang, Q.Z. Li, Synthesis of MCM-48 using mixed cationic-anionic surfactants as templates, Chem. Mater. 9 (1997) 2685.
[9] D. Zhao, P. Yang, N. Melosh, J. Feng, B.F. Chmelka, G.D. Stucky, Continuous mesoporous silica films with highly ordered large pore structures, Adv. Mater. 10 (1998) 1380.
[10] H. Yang, N. Coombs, I. Sokolov, G.A. Ozin, Registered growth of mesoporous silica films on graphite, J. Mater. Chem. 7 (1997) 1285.
[11] H. Miyata, K. Kuroda, Formation of a continuous mesoporous silica film with fully aligned mesochannels on a glass substrate, Chem. Mater. 12 (2000) 49.
[12] N. Nishiyama, A. Koide, Y. Egashira, K. Ueyama, Mesoporous MCM-48 membrane synthesized on a porous stainless steel support, Chem. Commun. (1998) 2147.
[13] R. Schmuhl, J. Sekulic, S. Roy Chowdhury, C.J.M. van Rijn, K. Keizer, A. van den Berg, J.E. ten Elshof, D.H.A. Blank, Si-compatible ion selective oxide interconnects with high tunability, Adv. Mater. 16 (2004) 900.
[14] K.J. Edler, S.J. Roser, Growth and characterization of mesoporous silica films, Int. Rev. Phys. Chem. 20 (2001) 387.
[15] C. Boissière, M.A.U. Martines, P.J. Kooyman, T.R. de Kruijff, A. Larbot, E. Prouzet, Ultrafiltration membrane made with mesoporous MSU-X silica, Chem. Mater. 15 (2003) 460.
[16] S. Roy Chowdhury, R. Schmuhl, K. Keizer, J.E. ten Elshof, D.H.A. Blank, Pore size and surface chemistry effects on the transport of hydrophobic and hydrophilic solvents through mesoporous γ-alumina and silica MCM-48, J. Membr. Sci. 225 (2003) 177.
[17] Y.S. Kim, S.-M. Yang, Preparation of continuous mesoporous silica thin film on a porous tube, Adv. Mater. 14 (2002) 1078.
[18] N. Nishiyama, H. Saputra, D.H. Park, Y. Egashira, K. Ueyama, Zirconium-containing mesoporous silica Zr-MCM-48 for alkali resistant filtration membranes, J. Membr. Sci. 218 (2003) 165.
[19] M. Klotz, A. Ayral, C. Guizard, L. Cot, Synthesis and characterization of silica membranes exhibiting an ordered mesoporosity. Control of the porous texture and effect on the membrane permeability, Sep. Purif. Tech. 25 (2001) 71.
[20] B.A. McCool, N. Hill, J. DiCarlo, W.J. DeSisto, Synthesis and characterization of mesoporous silica membranes via dip-coating and hydrothermal deposition techniques, J. Membr. Sci. 218 (2003) 55.
[21] D.H. Park, N. Nishiyama, Y. Egashira, K. Ueyama, Separation of organic/water mixtures with silylated MCM-48 silica membrane, Micropor. Mesopor. Mater. 66 (2003) 69.

[22] K. Nakagawa, H. Matsuyama, T. Maki, M. Teramoto, N. Kubota, Preparation of mesoporous silica membrane by solvent evaporation method for filtration application, Sep. Purif. Tech. 44 (2005) 145.
[23] C. Boissière, M.U. Martines, A. Larbot, E. Prouzet, On the specific filtration mechanism of a mesoporous silica membrane, prepared with non-connecting parallel pores, J. Membr. Sci. 251 (2005) 17.
[24] S. Roy Chowdhury, R. Schmuhl, K. Keizer, A. van den Berg, J.E. ten Elshof, D.H.A. Blank, Tailor-made nanostructured ion selective MCM-48 membranes, in: C.J. Brinker, M. Antonietti, Y. Lu, C. Bai (Eds.), Proceedings of the International Symposium on Self-Assembled Nanostructured Materials, Mat. Res. Soc. Proc. 775, Materials Research Society, Pittsburg, USA, 2003.
[25] I. Honma, H.S. Zhou, D. Kundu, A. Endo, Structural control of surfactant-templated hexagonal, cubic, and lamellar mesoporous silicate thin films prepared by spin-casting, Adv. Mater. 12 (2000) 1529.
[26] S. Roy Chowdhury, K. Keizer, J.E. ten Elshof, D.H.A. Blank, Effect of trace amounts of water on organic solvent transport through γ-alumina membranes with varying pore sizes, Langmuir 20 (2004) 4548.
[27] G.Z. Cao, J. Meijerink, H.W. Brinkman, A.J. Burggraaf, Permporometry study on the size distribution of active pores in porous ceramic membranes, J. Membr. Sci. 83 (1993) 221.
[28] D. Grosso, A.R. Balkenende, P.A. Albouy, A. Ayral, H. Amenitsch, F. Babonneau, Two-dimensional hexagonal mesoporous silica thin films prepared from block copolymers: detailed characterization and formation mechanism, Chem. Mater. 13 (2001) 1848.
[29] Y.F. Lu, R. Ganguli, C.A. Drewien, M.T. Anderson, C.J. Brinker, W.L. Gong, Y.X. Guo, H. Soyez, B. Dunn, M.H. Huang, J.I. Zink, Continuous formation of supported cubic and hexagonal mesoporous films by sol gel dip-coating, Nature 389 (1997) 364.
[30] M. Mulder, Basic Principles of Membrane Technology, Kluwer Academic Press, Dordrecht, The Netherlands, 1996.
[31] S. Roy Chowdhury, D.H.A. Blank, J.E. ten Elshof, Factors influencing the transport rate of short-chain alcohols through mesoporous γ-alumina membranes with varying pore sizes, J. Phys. Chem. B 109 (2005) 22141.
[32] A.F.M. Leenaars, A.J. Burggraaf, The preparation and characterization of alumina membranes with ultra-fine pores. Part 3. The permeability for pure liquids, J. Membr. Sci. 24 (1985) 245.